Journal of Ecological Engineering, 2026, 27(1), 150–164 https://doi.org/10.12911/22998993/209619 ISSN 2299–8993, License CC-BY 4.0

# Novel polyethersulfone membranes modified with polyvinylpyrrolidone and magnesium hydroxide: A study on performance and organic fouling mitigation

Mirna Rahmah Lubis<sup>1\*</sup>, Abrar Muslim<sup>1</sup>, Ryan Moulana<sup>1</sup>, Umi Fathanah, Syawaliah Muchtar<sup>1</sup>, Aulia Chintia Ambarita<sup>1</sup>

- <sup>1</sup> Department of Chemical Engineering, Syiah Kuala University, Jalan Syeh Abdur Rauf, Banda Aceh 23111, Indonesia
- \* Corresponding author's e-mail: mirna@usk.ac.id

#### **ABSTRACT**

This study explores the development and performance enhancement of polyethersulfone (PES) membranes through dual modification using polyvinylpyrrolidone (PVP) and magnesium hydroxide (Mg(OH)<sub>2</sub>). The objective was to investigate the impact of these additives on membrane permeability, rejection efficiency, and antifouling properties. Membranes were fabricated via non-solvent induced phase separation (NIPS) and characterized using FTIR, SEM, water contact angle (WCA) analysis, and filtration performance tests. Results showed that the PPM membrane achieved the highest pure water permeability (90.6 L/m²·h) due to improved porosity and hydrophilicity. FTIR analysis confirmed the presence of hydrophilic functional groups, while WCA measurements revealed a significant reduction in contact angle, indicating enhanced wettability. Although humic acid rejection slightly decreased to 70.5% in dual-modified membranes, the antifouling performance significantly improved, with a flux recovery ratio (FRR) of 87.2%. These findings demonstrate that the incorporation of PVP and Mg(OH)<sub>2</sub> into PES membranes synergistically improves water transport and fouling resistance. The study provides valuable insights for developing next-generation membranes suitable for complex water treatment applications, particularly in improving operational efficiency and durability.

Keyword: antifouling, membrane performance, magnesium hydroxide, polyethersulfone, polyvinylpyrrolidone.

## INTRODUCTION

Water pollution remains one of the most pressing global environmental challenges, with organic contaminants such as humic substances, proteins, and synthetic compounds posing serious threats to public health and aquatic ecosystems. As population growth and industrial expansion continue to strain freshwater resources, the need for efficient and sustainable water treatment technologies becomes increasingly urgent. Among the promising solutions, membranebased filtration systems have gained widespread attention due to their high contaminant removal efficiency, operational simplicity, and scalability. Polyethersulfone (PES) membranes frequently used in these systems owing to their

robust mechanical strength, thermal stability, and resistance to a broad range of chemical environments (Feng et al., 2021). However, the practical application of PES membranes is significantly hindered by organic fouling, a phenomenon that compromises membrane permeability, increases energy consumption, and shortens membrane lifespan (Kim et al., 2021).

Received: 2025.08.08 Accepted: 2025.09.17

Published: 2025.11.25

Organic fouling in PES membranes is predominantly caused by the adsorption of hydrophobic organic molecules onto the membrane surface. This leads to a progressive decline in membrane performance due to the formation of a fouling layer that obstructs water flow and encourages biofilm development (Sisay et al., 2023). The hydrophobic nature of PES exacerbates fouling by promoting strong

interactions between foulants and the membrane surface (Sousa et al., 2020). This irreversible adsorption not only reduces water permeability but also increases maintenance requirements, thereby affecting the economic feasibility of PES-based filtration systems (Kadavou et al., 2024; Nia et al., 2024; Fathanah et al., 2020). To address these issues, extensive research has been devoted to modifying PES membranes with hydrophilic additives to improve their antifouling properties and operational stability (Desiriani et al., 2023)

A key strategy for enhancing the antifouling performance of PES membranes involves the introduction of hydrophilic polymers and inorganic nanoparticles into the membrane matrix. Hydrophilic modification reduces the contact angle and increases surface energy, thereby forming a hydration layer that acts as a barrier against foulant deposition (Otitoju et al., 2018). Zwitterionic polymer brushes and hydrophilic copolymers have been reported to significantly lower protein adsorption and biofouling by improving membrane wettability (Jashrapuria and Singh, 2023; Liu et al., 2017). Similarly, additives such as polyethylene glycol and its derivatives enhance membrane hydrophilicity and permeability, contributing to improved overall filtration efficiency (Jie et al., 2020). Despite these advancements, the use of single-component additives often falls short of providing long-term stability and comprehensive fouling resistance.

Among various hydrophilic agents, polyvinylpyrrolidone (PVP) has emerged as a widely used polymer for PES membrane modification due to its excellent water solubility and ability to act as a pore-forming agent. Studies have shown that PVP incorporation results in membranes with enhanced porosity and lower contact angles, which translates into higher permeability and reduced fouling (Junaidi et al., 2019; Russo et al., 2021). Nevertheless, a critical limitation of PVP is its tendency to leach out during membrane operation, leading to a gradual decline in performance and membrane durability (Mavukkandy et al., 2016). On the other hand, magnesium hydroxide (Mg(OH)<sub>2</sub>) offers unique advantages as an inorganic additive. It introduces hydroxyl groups that contribute to hydrophilicity and also reinforces the membrane structure through hydrogen bonding (Fathanah et al., 2020; Abubakar et al., 2024). Mg(OH)2-modified membranes demonstrate improved stability and fouling

resistance, yet they often lack the permeability enhancements observed with polymeric additives (Umi Fathanah et al., 2024).

Recent studies have explored the synergistic use of organic and inorganic additives to overcome the limitations of single-component modifications. For instance, the combination of PVP with graphene oxide (GO) has been shown to significantly enhance antifouling performance and separation efficiency in PES membranes (Junaidi et al., 2019; Fathurrahman et al., 2021). Similar hybrid strategies involving titanium dioxide (TiO<sub>2</sub>) and carbon nanotubes (CNTs) alongside PVP have resulted in membranes with superior mechanical strength and water flux, as well as enhanced resistance to biofouling (Sarkar et al., 2017). These findings underscore the potential of combining organic polymers and inorganic nanoparticles to develop highperformance membranes tailored for specific water treatment applications.

Despite promising results from hybrid approaches, the combined application of PVP and Mg(OH)<sub>2</sub> in PES membranes remains relatively underexplored. The few existing studies suggest that such a combination may address the drawbacks of each component when used in isolation. While PVP enhances initial hydrophilicity and permeability, Mg(OH)2 contributes to structural integrity and long-term stability (Fathanah et al., 2022). Furthermore, optimization of the blending ratio and dispersion technique can lead to a well-balanced membrane with superior antifouling performance. The incorporation of both components has the potential to regulate phase inversion during membrane fabrication, resulting in a uniform and interconnected pore structure with enhanced permeability and fouling resistance.

Moreover, the use of the non-solvent induced phase separation (NIPS) method enables precise control over membrane morphology and additive distribution. Characterization techniques such as Fourier Transform Infrared Spectroscopy (FTIR), Scanning Electron Microscopy (SEM), water contact angle (WCA) measurement, and porosity analysis provide critical insights into the structural and functional transformations induced by PVP and Mg(OH)<sub>2</sub>. These techniques are essential for correlating chemical composition with filtration performance, particularly in terms of permeability, humic acid rejection, and flux recovery (Yang et al., 2022). Additionally, performance tests using

model foulants like humic acid offer practical evaluations of membrane resistance to organic fouling, a critical factor in real-world water treatment scenarios (Kim et al., 2021).

This study aims to systematically investigate the combined effects of PVP and Mg(OH)2 on the structural, hydrophilic, and antifouling properties of PES membranes. The novelty of the research lies in its focus on optimizing the synergistic interactions between organic and inorganic develop a high-performance additives to membrane that addresses the shortcomings of conventional modification strategies. Membranes will be fabricated using the NIPS method and characterized through a suite of analytical techniques, including FTIR, SEM, WCA, porosity, permeability, humic acid rejection, and flux recovery ratio assessments. By tailoring the membrane composition and fabrication parameters, this study seeks to identify an optimal formulation that maximizes permeability while maintaining effective contaminant rejection and long-term antifouling performance.

The outcomes of this research are expected to contribute significantly to the advancement of membrane technology for water treatment applications. Specifically, the findings will provide valuable insights into the design of next-generation PES membranes with improved durability, hydrophilicity, and resistance to organic fouling. These enhancements are critical for addressing the growing demand for clean water and supporting global sustainability goals through more efficient and reliable filtration technologies.

#### **EXPERIMENTAL**

# Chemicals

The fabrication of PES-based membranes in this study employed PES (E6020P, BASF) as the primary polymer due to its chemical resistance, thermal stability, and mechanical integrity, which are essential properties for water treatment applications (Hamzah et al., 2020). Polyvinylpyrrolidone (PVP) was utilized as a hydrophilic pore-forming additive to improve membrane wettability and porosity. Mg(OH)<sub>2</sub> was included as an inorganic modifier to enhance hydrophilicity and antifouling characteristics. Dimethylacetamide (DMAc, 99%, Sigma Aldrich) was used as the solvent, while deionized water functioned as

the non-solvent in the coagulation bath. Humic acid was selected as the model organic foulant to evaluate membrane rejection capabilities. All chemicals were of analytical grade and used without further purification.

## Membrane preparation

The membranes were fabricated using the non-solvent induced phase separation (NIPS) method, which is a widely recognized approach for producing asymmetric membranes with controlled porosity and structural integrity (Rahimpour et al., 2024). PES was dissolved in DMAc under continuous stirring to form a homogeneous base solution. Additives such as PVP, Mg(OH)<sub>2</sub>, and a combination of both were subsequently incorporated at designated concentrations and mixed for 24 hours to ensure uniform dispersion (Table 1). The resulting dope solutions were degassed using ultrasonication to eliminate entrapped air bubbles, which could otherwise compromise membrane structure.

Each prepared solution was cast on a glass substrate using a casting knife set at a wet thickness of 300  $\mu m$ . The cast films were then immersed in a deionized water coagulation bath at room temperature to initiate phase inversion. During this process, the solvent diffused out while water infiltrated the solution, leading to membrane solidification. Membranes remained in the bath for 24 hours to ensure complete removal of residual solvents, then were rinsed and stored in deionized water until further testing.

#### Membrane characterization

Functional group analysis by FTIR

Thermo Scientific iD5 ATR-Nicolet iS5 (FTIR) was used to identify the chemical composition of the membranes. Membrane samples were dried at 100 °C for 1 hour before analysis. The FTIR spectra were recorded in the range of 400–4000 cm<sup>-1</sup> to detect characteristic

**Table 1.** The polymer solution compositions

| Membrane<br>code | PES (%) | PVP (%) | Mg(OH) <sub>2</sub> (%) |
|------------------|---------|---------|-------------------------|
| P0               | 18      | 0       | 0                       |
| PP               | 18      | 1       | 0                       |
| PM               | 18      | 0       | 1                       |
| PPM              | 18      | 1       | 1                       |

functional groups in PES, PVP, and Mg(OH)<sub>2</sub>, particularly hydroxyl (-OH), carbonyl (C=O), and ether (C-O) groups, which indicate successful incorporation of additives.

## Morphological structure by SEM

SEM membrane morphology was observed using a field emission scanning electron microscope (FE-SEM, JSF-7500F, Jeol Co. Ltd.). Samples were freeze-dried, fractured in liquid nitrogen, and coated with osmium to enhance conductivity. SEM imaging at various magnifications enabled detailed examination of cross-sectional structures and pore formation influenced by additive types, corroborating their effects on membrane morphology (Wu et al., 2024).

## Porosity measurement

Membrane porosity was determined using the dry-wet weight method. The membranes were immersed in deionized water for 24 hours to ensure full saturation, then weighed in their wet state (W<sub>1</sub>). The membranes were subsequently dried in an oven at 50 °C until a constant weight (W<sub>2</sub>) was achieved. The porosity (%) was calculated using Equation 1.

$$\varepsilon = \frac{\left(\omega_{w} - \omega_{d}\right)}{\rho \times A \times l} \times 100\% \tag{1}$$

where:  $W_1$  and  $W_2$  are the wet and dry weights of the membrane (g),  $\rho$  is the density of water (1 g/cm<sup>3</sup>), A is the membrane surface area (cm<sup>2</sup>), and L is the membrane thickness (cm) (Umi Fathanah et al., 2025).

## Hydrophilicity by WCA

The hydrophilicity of the membranes was assessed by measuring the WCA using a Drop Master 300 contact angle meter (Kyowa Interface Science Co., Japan). Membrane samples were cut into 3  $\times$  1 cm strips, dried in a freeze dryer, and placed on the sample holder. A 1  $\mu L$  droplet of deionized water was dispensed onto the membrane surface, and the contact angle was recorded immediately after the droplet made contact. A lower contact angle indicated higher hydrophilicity. Each measurement was repeated five times at different locations on the membrane surface to ensure accuracy (Febriasari et al., 2021; Salim et al., 2022).

### Membrane performance evaluation

# Pure water permeability

The pure water permeability (PWP) of the membranes was evaluated using a dead-end filtration system. Membranes were compacted at 1 bar pressure for 1 hour before testing. Water flux was measured at 10-minute intervals under a constant transmembrane pressure (TMP) of 1 bar at room temperature. The pure water flux (J) was calculated using Equation 2.

$$J = \frac{\Delta V}{\Delta t A} \tag{2}$$

where: V is the volume of permeate collected (L), A is the effective membrane area (m<sup>2</sup>), and t is the filtration time (h) (Zhang et al., 2025).

# Humic acid rejection

The rejection performance of the membranes was assessed using a 50-ppm humic acid solution as the model organic pollutant. The filtration experiments were conducted in a dead-end filtration module at 2 bar pressure. The concentration of humic acid in the feed and permeate solutions was analyzed using a UV-Vis spectrophotometer at 254 nm. The rejection efficiency (R) was determined using Equation 3.

$$R = \frac{C_f - C_p}{C_f} \times 100\% \tag{3}$$

where:  $C_p$  and  $C_f$  are the concentrations of humic acid in the permeate and feed solutions, respectively.

## **Antifouling performance**

The antifouling behavior of the membranes was evaluated using the flux recovery ratio (FRR). The experiment was conducted in three steps: (1) initial pure water flux  $(J_1)$  measurement, (2) filtration of 50 ppm humic acid solution  $(J_2)$  at 2 bar for 60 minutes, (3) backwashing the membrane with deionized water for 20 minutes, followed by measuring the final pure water flux  $(J_3)$ . The flux recovery ratio (FRR) was calculated by Equation 4.

$$FRR = \frac{J_3}{J_1} \times 100\%$$
 (4)

#### **RESULT AND DISCUSSION**

#### Membrane characteristic

# Functional group

FTIR analysis was performed to confirm the successful incorporation of PVP and Mg(OH)<sub>2</sub> into the PES membrane matrix. Figure 1 presents the FTIR spectra of the unmodified PES membrane and those modified with varying compositions of PVP, Mg(OH)<sub>2</sub>, and their combination. In the spectrum of the pure PES (P0 membrane), characteristic peaks were observed at 1240 cm<sup>-1</sup> and 1105 cm<sup>-1</sup>, corresponding to the asymmetric and symmetric stretching vibrations of sulfone (SO<sub>2</sub>) groups, respectively. Additionally, the peak at 1485 cm<sup>-1</sup> was assigned to aromatic C=C stretching, which is typical for PES, confirming its intrinsic hydrophobicity.

Upon modification with PVP (PP membrane), an additional broad peak was detected around 1660 cm<sup>-1</sup>, corresponding to the C=O stretching of the lactam group in PVP. This confirms the successful incorporation of PVP into the membrane matrix, contributing to an increase in polar functional groups. Meanwhile, the membrane modified with Mg(OH)<sub>2</sub> (PM membrane) exhibited a decrease in peak intensity within the wavenumber range of 3000–3600 cm<sup>-1</sup> compared to the original unmodified membrane. This reduction in intensity indicates the presence of hydroxyl groups originating from the hydrophilic additive, Mg(OH)<sub>2</sub>.

The FTIR spectra of the PES membrane modified with PVP and Mg(OH)<sub>2</sub>(PPM membrane) exhibited both the C=O stretching peak from PVP and stretching vibration of hydroxyl (OH) groups from Mg(OH)<sub>2</sub>, confirming the successful incorporation of both additives. These findings indicate that the hydrophilic groups from PVP and Mg(OH)<sub>2</sub> were effectively integrated into the PES matrix, which is expected to enhance the membrane's hydrophilicity and antifouling properties. The impact of these hydrophilic groups on water contact angle (WCA) and overall membrane performance will be discussed later.

# Morphological structure

Figure 2 illustrates the cross-sectional SEM images of the fabricated membranes. P0 membrane exhibited a typical asymmetric structure with a dense skin layer and a limited number of finger-like macropores, a morphology arising from delayed demixing during phase inversion. With PVP modification, a notably more open structure was observed, characterized by elongated finger-like pores and increased pore density. This outcome affirms PVP's role as a pore-forming agent that accelerates solvent-nonsolvent exchange, thus enhancing porosity and water flux (Febriasari et al., 2021).

Conversely, membranes embedded with Mg(OH)<sub>2</sub> displayed a more compact morphology with shorter, narrower pores. The interaction

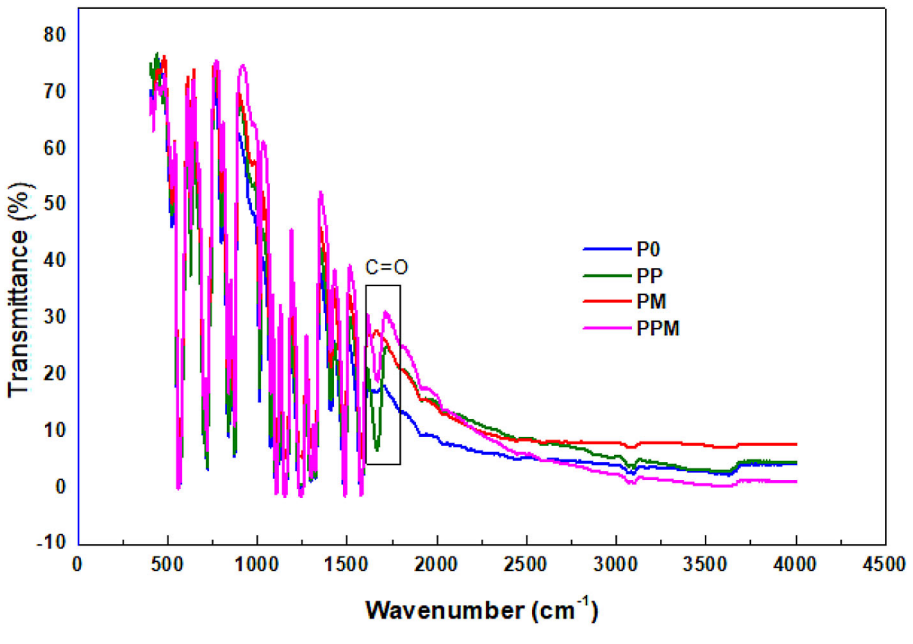


Figure 1. FTIR spectra of the prepared membranes

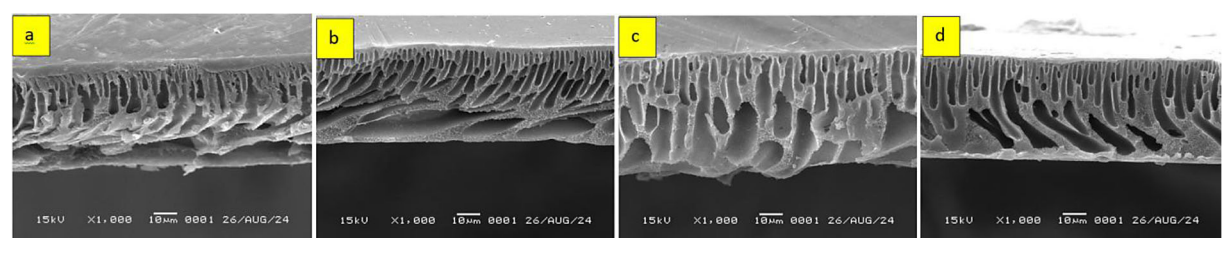


Figure 2. Cross-sectional structure of the membranes (a) P0; (b) PP; (c) PM; (d) PPM

between Mg(OH)<sub>2</sub> and PES likely retarded phase separation, contributing to this dense structure. This observation aligns with earlier findings suggesting that inorganic additives can alter the kinetics of phase inversion, influencing final pore architecture (Roslan et al., 2024; Chen et al., 2023). The PPM membrane, however, presented an optimal pore morphology with well-defined finger-like structures extending from the top to bottom layers. This morphology supports the notion of a synergistic effect, where PVP promotes macrovoid formation and Mg(OH)<sub>2</sub> contributes to structure regulation, producing membranes with high permeability and mechanical integrity.

## **Porosity**

The porosity results of the prepared membranes are summarized in Figure 3. The P0 membrane exhibited the lowest porosity (25%), consistent with its dense structure observed in SEM images. The incorporation of PVP increased porosity to 31%, confirming its role as a pore-forming agent that enhances macropore formation. In contrast, the PM membrane exhibited a slightly lower porosity (27%), likely due to the denser structure induced by Mg(OH)<sub>2</sub>, which slowed down phase separation and reduced pore formation.

In Figure 3 it could be observed that the highest porosity (35%) was observed in the PPM membrane, suggesting that the synergistic effect of PVP and Mg(OH)<sub>2</sub> enhanced phase separation dynamics, resulting in a more open and interconnected pore structure. Increased porosity is beneficial as it facilitates higher water flux and permeability. However, excessive porosity can compromise rejection efficiency, which will be further analyzed in the rejection study.

The porosity data strongly aligns with SEM observations. SEM images confirmed that PP membrane exhibited a higher density of macropores, correlating with increased porosity (Jalali et al., 2016). Similarly, the PPM membrane, which displayed the highest porosity

(35%), showed an enhanced porous network with well-distributed macropores in SEM images. Conversely, the denser morphology observed in PM membranes corresponded to slightly lower porosity values, reinforcing the role of Mg(OH)<sub>2</sub> in structural regulation.

The coherence between SEM and porosity measurements highlights how different dope solution compositions influence membrane architecture. A greater pore density and openness in SEM images correlate with higher porosity values, validating that PVP enhances pore formation, Mg(OH)<sub>2</sub> contributes to structural control, and their combination optimally balances porosity and mechanical stability. These findings confirm that the membrane fabrication approach effectively tailors pore architecture, optimizing permeability and antifouling performance for water treatment applications.

## Surface hydrophilicity

The WCA measurements for the different membranes are presented in Figure 4. A lower contact angle indicates greater hydrophilicity, which is desirable for minimizing membrane fouling. P0 membrane exhibited the highest contact angle (78°), confirming its inherent hydrophobicity. The addition of PVP reduced the WCA to 65°, indicating improved hydrophilicity due to the presence of hydrophilic functional groups in PVP. Similarly, the PM membrane showed a further reduction in WCA (58°), which can be attributed to the hydroxyl-rich nature of Mg(OH), particles, facilitating greater water interaction. The PPM membrane exhibited the lowest WCA (55°), demonstrating the highest hydrophilicity. This enhancement is due to the synergistic effect of PVP and Mg(OH), which introduce hydrophilic functional groups (-OH from Mg(OH), and C=O from PVP) to the membrane surface, increasing water affinity.

The lower WCA in PPM membranes is consistent with FTIR findings that revealed

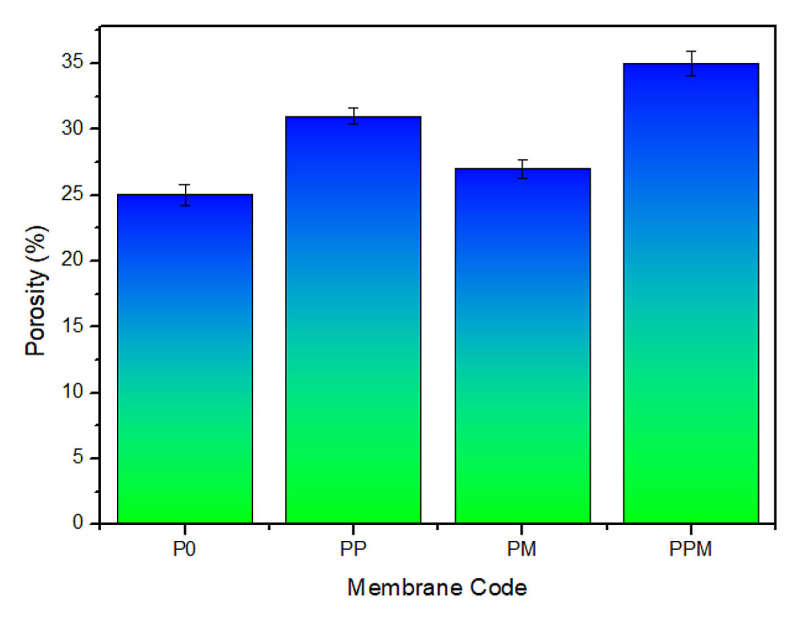


Figure 3. Porosity of the prepared membranes

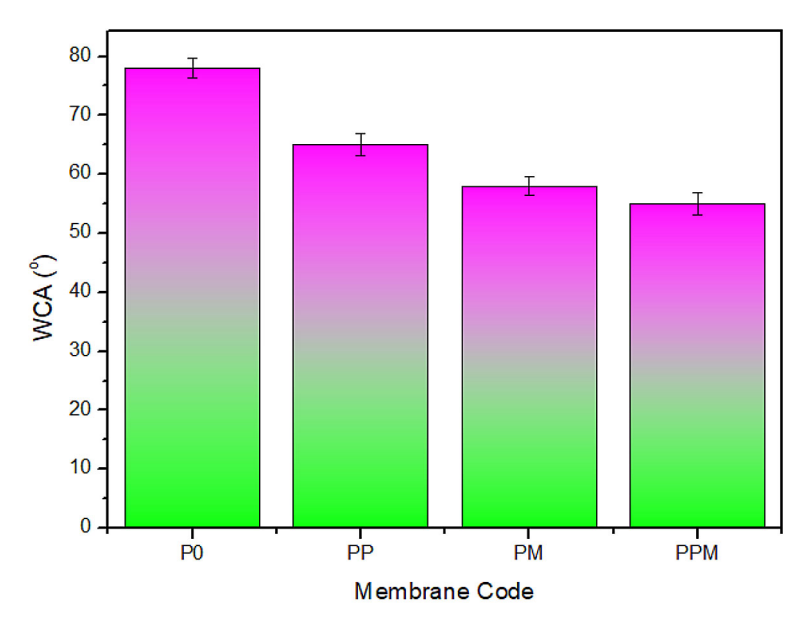


Figure 4. Water contact angle of the prepared membranes

the presence of polar functional groups. This strong correlation between FTIR peak intensity and WCA underscores the role of chemical functionality in enhancing hydrophilicity, which is a critical determinant of membrane antifouling performance (El-Zahhar et al., 2022; Irfan et al., 2015). Improved wettability helps prevent adhesion of organic foulants, thereby prolonging membrane lifespan and efficiency.

Together, the FTIR, SEM, porosity, and WCA analyses paint a coherent picture: blending PES with PVP and Mg(OH)<sub>2</sub> yields membranes with optimized pore structure and enhanced

surface hydrophilicity. This tailored design is expected to improve water permeability and reduce fouling tendencies, key requirements for efficient and sustainable membrane-based water treatment systems.

# Membrane performances

# Pure water permeability

The PWP results, as shown in Figure 5, demonstrate a clear relationship between membrane composition and water transport efficiency. The P0 membrane exhibited the lowest permeability

(17.5 L/m<sup>2</sup>·h), which increased significantly to 55.2 L/m<sup>2</sup>·h with the addition of PVP (PP membrane), confirming that enhanced porosity facilitated water transport. The PM membrane exhibited a higher flux (69.2 L/m<sup>2</sup>·h), suggesting that the presence of hydroxyl-rich Mg(OH)2 nanoparticles improved membrane wettability, thereby enhancing water permeability. The PPM membrane displayed the highest permeability (90.6 L/m<sup>2</sup>·h), indicating a synergistic effect between PVP-induced porosity and Mg(OH)2-enhanced hydrophilicity, which optimized water transport through the membrane structure. While increased permeability is beneficial for improving filtration efficiency, excessive porosity may reduce selectivity, an aspect that will be further analyzed in the rejection study.

WCA measurements further validate the influence of hydrophilicity on permeability. A lower WCA corresponds to higher hydrophilicity, allowing water molecules to spread more easily across the membrane surface, reducing resistance to flow. The unmodified PES membrane had the highest WCA (78°), confirming its hydrophobic nature and low permeability (17.5 L/m²·h). As PVP was introduced, WCA decreased to 65°, while permeability increased to 55.2 L/m²·h, demonstrating the direct impact of enhanced surface wettability on water transport. Similarly, Mg(OH)<sub>2</sub>-modified membranes exhibited a WCA reduction to 58°, contributing to an increase in

permeability (69.2 L/m<sup>2</sup>·h). The PPM membrane, with the lowest WCA (55°), achieved the highest permeability (90.6 L/m<sup>2</sup>·h), confirming that increased hydrophilicity significantly improved membrane efficiency.

Porosity plays an equally critical role in determining membrane permeability, as a higher porosity provides more pathways for water transport. The P0 membrane exhibited the lowest porosity (25%), which correlated with its low permeability, confirming that a dense structure restricts water flow. In contrast, PVP-modified membranes exhibited increased porosity (31%), which directly corresponded with the higher permeability of 55.2 L/m<sup>2</sup>·h, reinforcing the idea that the formation of additional pores improves water transport. The PM membrane had slightly lower porosity (27%) than the PVP-modified membrane, but still exhibited higher permeability (69.2 L/m<sup>2</sup>·h), suggesting that the improved hydrophilicity of Mg(OH), compensated for the slightly denser structure. The PPM membrane, with the highest porosity (35%), exhibited the highest permeability, demonstrating that both porosity and surface hydrophilicity work in tandem to optimize water flux.

The relationship between WCA, porosity, and permeability is clearly demonstrated in the PPM membrane, which exhibited the lowest WCA, highest porosity, and highest permeability. The synergistic effect of hydrophilic functional groups

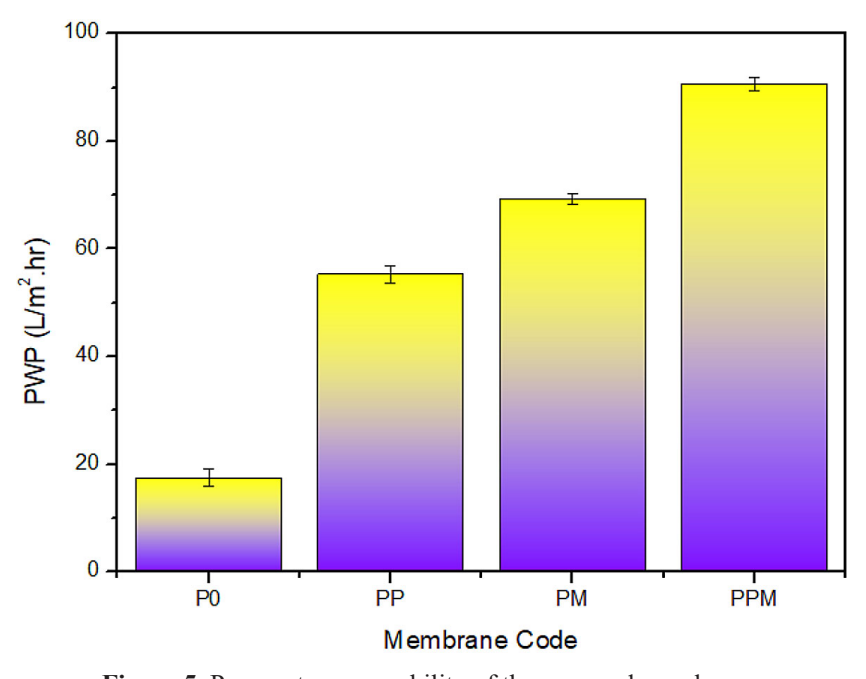


Figure 5. Pure water permeability of the prepared membranes

(from PVP and Mg(OH)<sub>2</sub>) and an optimized porous structure (from polymer blending and controlled phase inversion) contributed to superior water permeability. These results validate literature findings that increased porosity and hydrophilicity collectively enhance permeability (Roslan et al., 2024; Liu et al., 2016).

# Humic acid rejection

The rejection performance for humic acid is shown in Figure 6. The P0 membrane demonstrated the highest rejection rate of 77.1%, consistent with its compact structure and smaller pore size, which effectively blocked larger organic molecules. However, this came at the cost of reduced permeability. The PP membrane exhibited a slightly lower rejection (74.2%), likely due to the enlarged pore sizes associated with higher porosity, allowing partial humic acid penetration. The PM membrane retained 75.6% of humic acid, indicating a balanced performance due to moderate porosity and hydrophilic improvements.

The PPM membrane had the lowest rejection rate of 70.5%, attributable to its highly porous structure. While this composition maximized permeability, it did so at the expense of selectivity, echoing the well-known tradeoff between flux and rejection (Jo et al., 2016; Alkhattabi et al., 2025). This highlights the importance of optimizing additive ratios to

balance transport efficiency with contaminant filtration, especially in wastewater treatment applications (Man et al., 2020).

Scanning electron microscopy (SEM) images support this interpretation. The P0 membrane showed a dense morphology with limited fingerlike macropores, aligning with its low permeability and high rejection. The PP membrane displayed a more open structure with pronounced fingerlike pores, improving permeability but slightly compromising rejection. The PM membrane had a denser structure compared to PP membrane, contributing to moderate rejection enhanced water transport. In PPM membrane, SEM revealed a well-developed network of macropores, responsible for its excellent water flux and decreased rejection.

This inverse correlation between permeability and rejection efficiency reflects the structural-functional balance in membrane engineering. The PPM membrane exemplifies trade-off, achieving superior permeability while moderately reducing filtration performance. Thus, membrane design must consider specific application requirements, tailoring porosity and hydrophilicity to achieve optimal operational outcomes.

In this study, humic acid was selected as the model contaminant because it is one of the most representative fractions of natural organic matter (NOM) commonly present in surface waters and

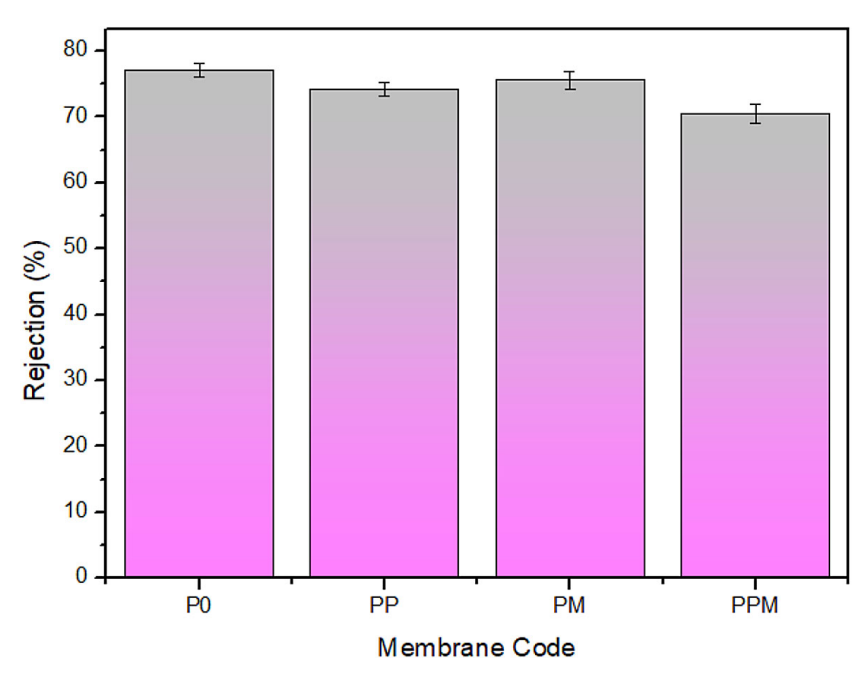


Figure 6. Humic acid rejection of the prepared membranes

is widely used as a benchmark foulant in membrane performance evaluation (Xie et al., 2019; Kywe et al., 2022). While humic acid rejection provides valuable insight into organic fouling resistance, it does not encompass the full spectrum of contaminants encountered in practical applications. For example, proteins and polysaccharides, which are abundant in biological wastewater, are known to strongly adhere to hydrophobic surfaces; increasing membrane hydrophilicity reduces this adhesion by forming a hydration layer that repels foulants. Similarly, oil emulsions and other hydrophobic organics have been shown to cause severe fouling in unmodified membranes, but hydrophilic surfaces mitigate this effect by preventing droplet adsorption and enhancing flux recovery (Sisay et al., 2023). For inorganic foulants such as heavy metals or colloidal silica, the increased porosity and hydrophilicity of modified membranes improve cleanability and flux recovery, thereby reducing irreversible fouling (Mazumdel et al., 2020). Thus, while humic acid served as a relevant model foulant in this study, the structural and surface modifications introduced are anticipated to enhance performance against a broader range of organic and inorganic contaminants, although further systematic evaluations remain necessary.

## **Antifouling mitigation**

The antifouling performance of the membranes was evaluated using the flux recovery ratio (FRR), a widely accepted metric for assessing the ability of membranes to regain permeability following exposure to fouling agents. As depicted in Figure 7, the P0 membrane exhibited the lowest FRR (42.6%), indicative of a high degree of irreversible fouling. This result aligns with its hydrophobic character, which facilitates foulant adhesion. In contrast, membranes modified with hydrophilic agents showed markedly higher FRR values, with PP membrane and PM membrane achieving FRRs of 67.8% and 60.4%, respectively. The highest FRR (87.2%) was obtained for the PPM membrane, demonstrating a superior resistance to fouling due to the synergistic effects of both PVP and Mg(OH)<sub>2</sub>.

The enhancement in antifouling capacity is directly related to modifications in membrane surface chemistry and structure, which were characterized using FTIR and WCA measurements. FTIR spectra confirmed the

incorporation of functional groups associated with increased hydrophilicity. For instance, the PP membrane displayed an additional absorption peak at approximately 1660 cm<sup>-1</sup>, corresponding to the carbonyl (C=O) stretching vibration from PVP, indicating the presence of polar groups. Similarly, the PM membrane exhibited a peak around 3000-3600 cm<sup>-1</sup>, indicating the presence of OH bonds from Mg(OH), which are likely associated with hydroxyl groups contributing to hydrophilic properties (Acarer et al., 2024). The PPM membrane showed both these peaks, confirming the successful integration of both additives and suggesting the formation of a more hydrophilic surface, which is beneficial in mitigating organic fouling.

The hydrophilic nature of the membrane surfaces, quantified by WCA measurements, further supports these findings. The WCA of the P0 membrane was measured at 78°, while that of PP membrane, PM membrane, and PPM membrane decreased to 65°, 58°, and 55°, respectively. These lower WCA values signify enhanced surface wettability, which facilitates the formation of hydration layers on the membrane surface, thereby reducing foulant adhesion (Irfan et al., 2015) (Febriasari et al., 2021). The data clearly demonstrate that a decrease in WCA correlates with an increase in FRR, emphasizing the critical role of surface hydrophilicity in antifouling performance.

The correlation between FTIR-detected functional groups, WCA, and FRR values is consistent with findings in membrane science literature. Membranes exhibiting functional groups such as hydroxyl (-OH) or carbonyl (C=O) have demonstrated enhanced antifouling capabilities by promoting hydrophilicity and forming hydration barriers (Salim et al., 2022; Liu et al., 2019). The PPM membrane, with dual-functional modification, benefitted from both the structural attributes of PVP and the hydrophilic contribution of Mg(OH)<sub>a</sub>. The resulting surface chemistry effectively minimized foulant-membrane interactions and allowed better cleaning, leading to an exceptional FRR of 87.2%.

The high flux recovery ratio (FRR) of 87.2% provide indirect evidence of the long-term stability of the modified membranes, as it indicates that the PPM membrane can effectively recover permeability after a fouling-cleaning cycle, suggesting resilience under repeated

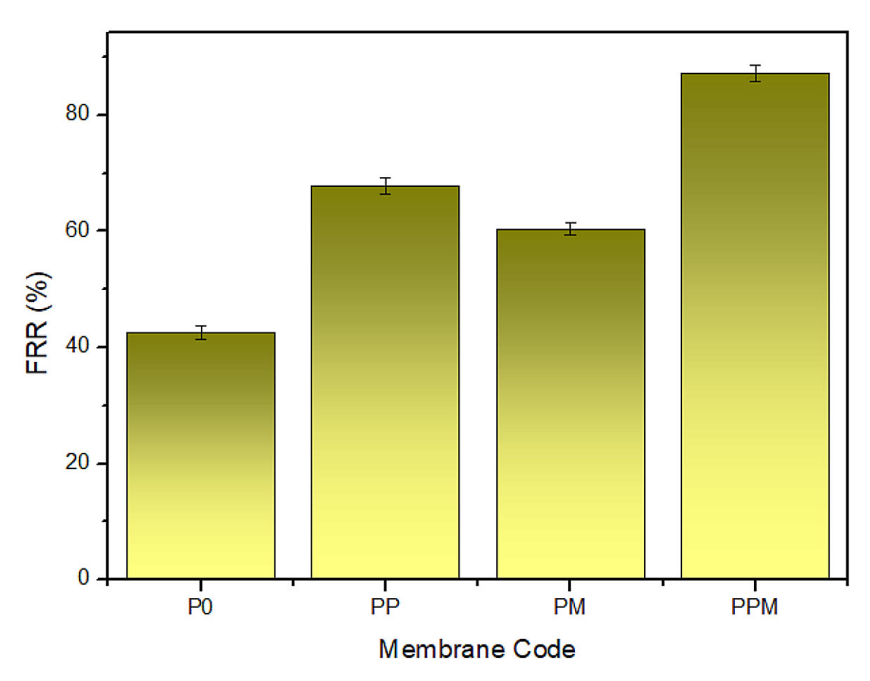


Figure 7. FRR of the prepared membranes

operation. In addition, SEM analysis revealed a well-distributed pore structure in the PPM membrane, which is less prone to compaction under pressure compared to highly porous single-additive systems. The FTIR spectra also confirmed the presence of stable hydrophilic functional groups (-OH from Mg(OH), and C=O from PVP) covalently or strongly associated with the PES matrix, which reduces the likelihood of rapid additive leaching. Together, these findings suggest that the dual incorporation of PVP and Mg(OH), enhances not only the initial performance but also the potential operational stability of the membrane, even though extended continuous tests will be required to fully confirm long-term durability.

This observation aligns with earlier findings that dual modification strategies involving both organic and inorganic additives can synergistically enhance long-term membrane performance. Studies have shown that such dual-modified membranes not only improve antifouling resistance but also maintain structural stability and performance over prolonged filtration operations, especially under complex feed conditions (Lakshmanan et al., 2025; Man et al., 2020). The high FRR achieved by the PPM membrane validates this approach, indicating its potential suitability for challenging filtration scenarios such as wastewater treatment or industrial effluent purification.

These results underscore the pivotal role of membrane surface modification in mitigating fouling, with FTIR, WCA, and FRR providing complementary insights into the mechanisms at play. The combined use of PVP and Mg(OH)<sub>2</sub> not only improved membrane hydrophilicity but also enhanced recovery performance after fouling, thereby addressing one of the most critical challenges in membrane filtration systems.

# Performance comparison

As shown in Table 2, several studies have investigated hybrid modifications of PES/PVP membranes using inorganic nanoparticles. For instance, PVP + TiO<sub>2</sub> systems have demonstrated a two- to three-fold increase in permeability (55– 66 L·m<sup>-2</sup>·h<sup>-1</sup>) while maintaining high humic acid rejection (~95–96%) and achieving flux recovery ratios of 83-89%. Incorporation of graphene oxide (GO) into PES/PVP membranes produced even greater permeability improvements, with reported fluxes of ~150.2 L·m<sup>-2</sup>·h<sup>-1</sup> (about eight times pristine PES) and Pb2+ rejection enhanced from 38.9% to 80.6%. Similarly, PVP-functionalized carbon nanotubes (CNTs) significantly improved antifouling, yielding ~93.4% BSA rejection and an FRR of ~81.7%. In comparison, the dual PVP + Mg(OH), (PPM)membranes developed in this study achieved a flux of 90.6 L·m<sup>-2</sup>·h<sup>-1</sup> (five times pristine PES)

| Hybrid system (Additives)                          | Pure water flux /<br>Permeability                             | Rejection (model contaminant)                       | Antifouling (FRR)                       | Reference               |
|--|---|---|---|-------------------------|
| PES/PVP + TiO <sub>2</sub>                         | 55–66 L·m <sup>-2</sup> ·h <sup>-1</sup> (≈2–3× pristine PES) | ~95–96% (Humic Acid)                                | 83–89% (vs 77% pristine PES)            | Ahmad et al., 2022      |
| PES/PVP + GO                                       | ~150.2 L·m <sup>-2</sup> ·h <sup>-1</sup> (≈8× pristine PES)  | ~80.6% (Pb <sup>2+</sup> ions) vs<br>38.9% pristine | Good fouling resistance (easy cleaning) | Poolachira et al., 2022 |
| PES/PVP + CNT                                      | (Not directly reported for water flux)                        | ~93.4% (BSA, 66 kDa<br>protein)                     | ~81.7% FRR; ~80% fouling reversible     | Irfan et al., 2015      |
| PES/PVP + Mg(OH) <sub>2</sub><br>(PPM, this study) | 90.6 L·m⁻²·h⁻¹ (≈5×<br>pristine PES)                          | 70.5% (Humic Acid)                                  | 87.2% FRR                               | This study              |

**Table 2.** Performance comparison with other PVP-based hybrid additive systems

and an FRR of 87.2%, which is higher than most reported systems. Although humic acid rejection (70.5%) was lower than in TiO<sub>2</sub> or CNT-based hybrids, the PPM membranes provide a strong balance between permeability and antifouling, underscoring their potential for practical water treatment applications where fouling resistance and operational stability are critical.

#### **CONCLUSIONS**

This study systematically evaluated the synergistic effects of PVP and Mg(OH)2 as dual additives in polyethersulfone membranes fabricated via non-solvent induced phase separation. The modified membranes demonstrated significant enhancements in water permeability, rejection performance, and antifouling resistance compared to unmodified PES. Among all variations, the PPM membrane displayed the highest pure water permeability of 90.6 L/m<sup>2</sup>.h, attributable to improved porosity and surface hydrophilicity. Although it showed a moderate decline in humic acid rejection (70.5%), the membrane's antifouling capability improved markedly, as indicated by a flux recovery ratio of 87.2%. The study highlighted clear correlations between structural characteristics (WCA, FTIR signatures) and membrane performance. FTIR confirmed the integration of hydrophilic groups (C=O and OH) while WCA analysis revealed lower contact angles for modified membranes, demonstrating increased wettability. These attributes collectively contributed to enhanced antifouling behavior. Overall, this study validates that organic-inorganic dual-additive strategies can be effectively employed to tailor permeability and antifouling properties of PES membranes. Future research may focus on optimizing additive concentrations, conducting extended long-term stability tests, and benchmarking performance under diverse real wastewater conditions to further enhance selectivity and durability.

# Acknowledgments

The authors would like to express their gratitude to the Ministry of Higher Education, Science, and Technology of the Republic of Indonesia for the Regular Fundamental Research (PFR) grant (No. 646/UN11.2.1/PG.01.03/SK/DRTPM/2024), and the Process Technology Laboratory for laboratory facilities.

#### **REFERENCES**

- Abubakar, A., Fathanah, U., Lubis, M. R., Muchtar, S., Rahmania, T. P., Syarwani, I. (2024). Effect of adding Mg(OH)<sub>2</sub> additives to polyethersulfone (PES) hydrophobic membranes. *Materials Science Forum*, 1137, 11–19. https://doi.org/10.4028/p-odZas7
- Acarer, S., Pir, İ., Tüfekci, M., Öz, N., Tüfekçi, N. (2024). Effect of promising sustainable nano-reinforcements on polysulfone/polyvinylpyrrolidonebased membranes: Enhancing mechanical properties and water filtration performance. *Polymers*, 16(24), 3531. https://doi.org/10.3390/polym16243531
- Ahmad, A. L., Che Lah, N. F., Norzli, N. A., Pang, W. Y. (2022). A contrastive study of self-assembly and physical blending mechanism of TiO<sub>2</sub> blended polyethersulfone membranes for enhanced humic acid removal and alleviation of membrane fouling. *Membranes*, 12(2), 162. https://doi.org/10.3390/ membranes12020162
- Alkhattabi, L., Harun, N. Y., Zeeshan, M., Waqas, S., Hanbazazah, A. S. (2025). Gradient cross-linking graphene oxide–integrated nanofiltration polyvinylpyrrolidone membrane for polycyclic aromatic hydrocarbons removal. *International Journal of Polymer Science*, 2025(1). https://doi.org/10.1155/ijps/1822074
- Chen, L., Zhao, L., Ding, K. (2023). Preparation and Characterization of PSF/SPSF Blended

- Ultrafiltration Membranes. *Pigment & Resin Technology*, *53*(6), 1100–1110. https://doi.org/10.1108/prt-05-2023-0040
- Desiriani, R., Susanto, H., Istirokhatun, T., Lin, Y., Aryanti, N., Abriyanto, H., Saputra, H., Matsuyama, H. (2023). Preparation of polyethersulfone ultrafiltration membrane coated natural additives toward antifouling and antimicrobial agents for surface water filtration. *Journal of Environmental Chemical Engineering*. https://doi.org/10.1016/j. jece.2023.111797
- El-Zahhar, A. A., Alghamdi, M. M., Alshahrani, N. M., Awwad, N. S., Idris, A. M. (2022). Development of composite thin-film nanofiltration membranes based on polyethersulfone for water purification. *Journal of Polymers and the Environment*, 30(10), 4350–4361. https://doi.org/10.1007/ s10924-022-02499-x
- Fathanah, U, Machdar, I., Riza, M., Arahman, N., Wahab, M. Y., Muchtar, S., Rosnelly, C. M., Mulyati, S., Syamsuddin, Y., Juned, S., Razi, F. (2022). Effect of hybrid Mg(OH)<sub>2</sub>/Chitosan on the hydrophilicity and antifouling of polyethersulfone (PES) membrane. *Rasayan Journal of Chemistry*, 15(2), 813–823. https://doi.org/10.31788/RJC.2022.1526582 This
- Fathanah, U., Machdar, I., Riza, M., Arahman, N., Yusuf, M., Bilad, M. R., Abdul, N., Nordin, H., Pes, P. (2020). Enhancement of antifouling of ultrafiltration polyethersulfone membrane with hybrid Mg ( OH) 2 / chitosan by polymer blending graphical abstract keywords. *Journal of Membrane Science* and Research, 6, 375–382. https://doi.org/10.22079/ JMSR.2020.124107.1365
- 10. Fathanah, U., Muchtar, S., Aprilia, S., Lubis, M. R., Mulyati, S., Yusuf, M. (2024). Unlocking synergies of Mg(OH)<sub>2</sub> and rice husk silica as dual additives for tailored pore properties, selectivity, and antifouling performances of PES membrane. *South African Journal of Chemical Engineering*, 48(January), 22–29. https://doi.org/10.1016/j.sajce.2024.01.004
- Fathanah, U., Rosnelly, C. M., Zuhra, Z., Muchtar, S., Razi, F., Rinaldi, W., Syamsuddin, Y. (2025). Integrated approach to elevating PES membrane performance with a dynamic silica and chitosan additive duo. South African Journal of Chemical Engineering, 53(April), 1–11. https://doi.org/10.1016/j. sajce.2025.04.007
- 12. Fathurrahman, A., Arisandi, R., Fahrina, A., Arahman, N., Razi, F. (2021). Filtration performance of polyethersulfone (PES) composite membrane incorporated with organic and inorganic additives. 1087(1), 12049. https://doi.org/10.1088/1757-899X/1087/1/012049
- Febriasari, A., Huriya, Ananto, A. H., Suhartini, M., Kartohardjono, S. (2021). Polysulfone–polyvinyl

- pyrrolidone blend polymer composite membranes for batik industrial wastewater treatment. *Membranes*, *11*(1), 66. https://doi.org/10.3390/membranes11010066
- 14. Feng, Y., Feng, Y., Chung, T.-S. (2021). Fabrication and applications of polyethersulfone hollow fiber membranes 315–332. Elsevier. https://doi.org/10.1016/B978-0-12-821876-1.00012-3
- Hamzah, N., Johary, F., Rohani, R., Sharifuddin, S. S., Isa, M. H. (2020). Development of polyether-sulfone (PES)/reduced graphene oxide nanocomposite nanofiltration membrane. *Malaysian Journal of Fundamental and Applied Sciences*, 16(4), 418–421. https://doi.org/10.11113/MJFAS.V16N4.1613
- 16. Irfan, M., Basri, H., Irfan, M., Lau, W. (2015). An acid functionalized MWCNT/PVP nanocomposite as a new additive for fabrication of an ultrafiltration membrane with improved anti-fouling resistance. *RSC Advances*, 5(116), 95421–95432. https://doi.org/10.1039/c5ra11344j
- 17. Jafar Mazumder, M. A., Raja, P. H., Isloor, A. M., Usman, M., Chowdhury, S. H., Ali, S. A.,... Al-Ahmed, A. (2020). Assessment of sulfonated homo and copolyimides incorporated polysulfone ultrafiltration blend membranes for effective removal of heavy metals and proteins. *Scientific Reports*, 10(1), 7049.
- 18. Jalali, A., Shockravi, A., Vatanpour, V., Hajibeygi, M. (2016). Preparation and characterization of novel microporous ultrafiltration PES membranes using synthesized hydrophilic polysulfide-amide copolymer as an additive in the casting solution. *Microporous and Mesoporous Materials*, 228, 1–13. https://doi.org/10.1016/j.micromeso.2016.03.024
- Jashrapuria, K., Singh, S. P. (2023). Zwitterionic polymer brush functionalized graphene oxide blended polyethersulfone membrane with enhanced performance and anti-biofouling properties. *Journal* of Membrane Science. https://doi.org/10.1016/j. memsci.2023.122032
- 20. Jie, S. J., Seng, O. B., Ting, L. L. H., Yao, S. J. (2020). Development of Antifouling Poly(vinylidene Fluoride) Ultrafiltration Membrane with the Addition of Polyethylene Glycol as Additive. 463(1), 12178. https://doi.org/10.1088/1755-1315/463/1/012178
- 21. Jo, Y. J., Choi, E. Y., Choi, N., Kim, C. K. (2016). Antibacterial and hydrophilic characteristics of poly(ether Sulfone) composite membranes containing zinc oxide nanoparticles grafted with hydrophilic polymers. *Industrial & Engineering Chemistry Research*, 55(28), 7801–7809. https://doi.org/10.1021/acs.iecr.6b01510
- 22. Junaidi, N. F. D., Othman, N. H., Shahruddin, M. Z., Alias, N. H., Lau, W. J., Ismail, A. F. (2019). Effect of graphene oxide (GO) and polyvinylpyrollidone (PVP) additives on the hydrophilicity of composite polyethersulfone (PES) membrane.

- Malaysian Journal of Fundamental and Applied Sciences, 15(3), 361–366. https://doi.org/10.11113/MJFAS.V15N3.1209
- 23. Kadavou, D., Arumugham, T., Tizani, L., Hasan, S. W. (2024). Enhanced antifouling and separation capabilities of polydopamine@Ce-MOF functionalized PES ultrafiltration membrane. *Npj Clean Water*. https://doi.org/10.1038/s41545-024-00302-z
- 24. Kim, H., Shim, I., Zhan, M. (2021). Chemical enhanced backwashing for controlling organic fouling in drinking water treatment using a novel hollow-fiber polyacrylonitrile nanofiltration membrane. *Applied Sciences*, 11(15), 6764. https://doi. org/10.3390/APP11156764
- Kim, S., Alayande, A. B., Nguyen, T.-T. (2021).
  Organic and biological fouling. https://doi. org/10.2166/9781780409863\_0125
- 26. Kywe, P. P., Ratanatamskul, C. (2022). Direct contact membrane distillation for treatment of mixed wastewater of humic acid and reactive dye: Membrane flux decline and fouling analysis. ACS omega, 7(42), 37846–37856. https://doi.org/10.1021/acsomega.2c04932
- 27. Lakshmanan, S., Ponnaiyan, P., Jeganathan, K., Gopalakrishnan, N. (2025). Fabrication and characterization of GO-TiO<sub>2</sub> embedded PSF-PVP polymer composite membranes for enhanced membrane characteristics and antifouling performance. *Physica Scripta*, 100(4), 45937. https://doi.org/10.1088/1402-4896/adbe06
- 28. Liu, Caihong, de Faria, A. F., Ma, J., Elimelech, M. (2017). Mitigation of biofilm development on thin-film composite membranes functionalized with zwitterionic polymers and silver nanoparticles. *Environmental Science & Technology*, *51*(1), 182–191. https://doi.org/10.1021/ACS.EST.6B03795
- 29. Liu, Chao, Guo, Y., Zhang, J., Tian, B., Lin, O., Liu, Y., Zhang, C. (2019). Tailor-made high-performance reverse osmosis membranes by surface fixation of hydrophilic macromolecules for wastewater treatment. *RSC Advances*, 9(31), 17766–17777. https://doi.org/10.1039/c9ra02240f
- 30. Liu, J., Zhong, Z., Ma, R., Zhang, W., Li, J. (2016). Development of high-antifouling PPSU ultrafiltration membrane by using compound additives: preparation, morphologies, and filtration resistant properties. *Membranes*, 6(2), 35. https://doi.org/10.3390/membranes6020035
- 31. Man, H. C., Abba, M. U., Abdulsalam, M., Azis, R. S., Idris, A. I., Hamzah, M. H. (2020). Utilization of nano-TiO<sub>2</sub> as an influential additive for complementing separation performance of a hybrid PVDF-PVP hollow fiber: Boron removal from leachate. *Polymers*, 12(11), 2511. https://doi.org/10.3390/polym12112511

- 32. Mavukkandy, M. O., Bilad, M. R., Giwa, A., Hasan, S. W., Arafat, H. A. (2016). Leaching of PVP from PVDF/PVP blend membranes: impacts on membrane structure and fouling in membrane bioreactors. *Journal of Materials Science*, 51(9), 4328–4341. https://doi.org/10.1007/S10853-016-9744-7
- 33. Nia, H. R., Aroujalian, A., Salimi, P. (2024). Antifouling performance enhancement of PES membranes using hydrophilic nanoparticles of poly(dopamine-acrylate) for oil/water separation. *Journal of Environmental Chemical Engineering*. https://doi.org/10.1016/j.jece.2024.112797
- 34. Otitoju, T. A., Ahmad, A. L., Ooi, B. S. (2018). Recent advances in hydrophilic modification and performance of polyethersulfone (PES) membrane via additive blending. *RSC Advances*, *8*(40), 22710–22728. https://doi.org/10.1039/c8ra03296c
- 35. Poolachira, S., Velmurugan, S. (2022). Efficient removal of lead ions from aqueous solution by graphene oxide modified polyethersulfone adsorptive mixed matrix membrane. *Environmental Research*, 210, 112924. https://doi.org/10.1016/j.envres.2022.112924
- 36. Rahimpour, A., Kebria, M. R. S., Firouzjaei, M. D., Mozafari, M. R., Elliott, M., Sadrzadeh, M. (2024). Nonsolvent-induced Phase Separation 1–36. Elsevier BV. https://doi.org/10.1016/ b978-0-323-95628-4.00009-4
- 37. Roslan, R. A., Lau, W. J., Nawi, N. S. M., Nxumalo, E. N., Ismail, A. F. (2024). Enhancing properties of PSF membrane via a simple two-step coating of PDA and PVP for separating oil/water emulsions. *Journal of Chemical Technology & Biotechnology*, 100(1), 37–49. https://doi.org/10.1002/jctb.7752
- Russo, F., Bulzomì, M., Nicolo, E. Di, Ursino, C., Figoli, A. (2021). Enhanced Anti-Fouling Behavior and Performance of PES Membrane by UV Treatment. 9(2), 246. https://doi.org/10.3390/PR9020246
- Salim, A., Abbas, M. A., Khan, I. A., Khan, M. K., Javaid, F., Mushtaq, S., Batool, M., Yasir, M., Khan, A. L., Khan, A.-R., Deen, K. M., Ahmad, N. M. (2022). Graphene oxide incorporated polyether sulfone nanocomposite antifouling ultrafiltration membranes with enhanced hydrophilicity. *Materials Research Express*, 9(7), 75503. https://doi.org/10.1088/2053-1591/ac81a3
- Sarkar, S., Sarkar, A., Bhattacharjee, C. (2017).
  Nanotechnology-based Membrane-separation Process for Drinking Water Purification 355–389.
   Academic Press. https://doi.org/10.1016/B978-0-12-804300-4.00010-1
- 41. Sisay, E. J., Al-Tayawi, A. N., László, Z., Kertész, S. (2023). Recent advances in organic fouling control and mitigation strategies in membrane separation processes: A review. *Sustainability*, *15*(18), 13389. https://doi.org/10.3390/su151813389

- 42. Sousa, M. R. S., Lora-García, J., López-Pérez, M.-F., Heran, M. (2020). Identification of foulants on polyethersulfone membranes used to remove colloids and dissolved matter from paper mill treated effluent. *Water*, 12(2), 365. https://doi.org/10.3390/W12020365
- 43. Wu, J., Xiao, M., Quezada-Renteria, J. A., Hou, Z., Hoek, E. M. V. (2024). Sample Preparation Matters: Scanning Electron Microscopic Characterization of Polymeric Membranes. https://doi.org/10.2139/ssrn.4705204
- 44. Xie, P., Murdoch, L. C., Ladner, D. A. (2019). Mitigating membrane fouling with sinusoidal spacers. *Desalination and Water Treatment*, 168, 56-64.
- 45. Yang, D., Rong, P., Jiang, C., Liu, P., Jiang, M., Zhang, S. (2022). Fabrication of polyarylate-based porous membranes from nonsolvent-induced phase separation process and related permeability and filterability characterizations. *ACS Applied Polymer Materials*, *5*(1), 968–982. https://doi.org/10.1021/acsapm.2c01896
- 46. Zhang, Z., Wang, B. Y., Zhang, X., Wang, Z., Ding, Q., Liu, X., Wang, L., Li, Z., Liu, Y. (2025). Design and performance of hydrophilic poly(Aryl Ether Oxadiazole) ultrafiltration membranes with good antifouling properties. *Journal of Applied Polymer Science*, 142(28). https://doi.org/10.1002/app.57142